2013

Lytic cycle: A defining process in oncolytic virotherapy

Yujie Wang

Junjie Wei

Jianjun Paul Tian
William & Mary

Yujie Wang

Recommended Citation

Wang, Y., Tian, J. P., & Wei, J. (2013). Lytic cycle: A defining process in oncolytic virotherapy. Applied Mathematical Modelling, 37(8), 5962-5978.

Applied Mathematical Modelling 37 (2013) 5962–5978

Contents lists available at SciVerse ScienceDirect

Applied Mathematical Modelling

journal homepage: www.elsevier.com/locate/apm

Lytic cycle: A defining process in oncolytic virotherapy

Yujie Wang [a,c], Jianjun Paul Tian [b], Junjie Wei [a,*]

[a] Department of Mathematics, Harbin Institute of Technology, Harbin, Heilongjiang 150001, PR China
[b] Department of Mathematics, The College of William and Mary, Williamsburg, VA 23187, USA
[c] Department of Mathematics, Jilin Normal University, Siping 136000, PR China

ARTICLE INFO

Article history:
Received 22 February 2012
Received in revised form 22 November 2012
Accepted 18 December 2012
Available online 27 December 2012

Keywords:
Oncolytic virotherapy
Lytic cycle
Burst size
Global stability
Bifurcation

ABSTRACT

The viral lytic cycle is an important process in oncolytic virotherapy. Most mathematical models for oncolytic virotherapy do not incorporate this process. In this article, we propose a mathematical model with the viral lytic cycle based on the basic mathematical model for oncolytic virotherapy. The viral lytic cycle is characterized by two parameters, the time period of the viral lytic cycle and the viral burst size. The time period of the viral lytic cycle is modeled as a delay parameter. The model is a nonlinear system of delay differential equations. The model reveals a striking feature that the critical value of the period of the viral lytic cycle is determined by the viral burst size. There are two threshold values for the burst size. Below the first threshold, the system has an unstable trivial equilibrium and a globally stable virus free equilibrium for any nonnegative delay, while the system has a third positive equilibrium when the burst size is greater than the first threshold. When the burst size is above the second threshold, there is a functional relation between the bifurcation value of the delay parameter for the period of the viral lytic cycle and the burst size. If the burst size is greater than the second threshold, the positive equilibrium is stable when the period of the viral lytic cycle is smaller than the bifurcation value, while the system has orbitally stable periodic solutions when the period of the lytic cycle is longer than the bifurcation value. However, this bifurcation value becomes smaller when the burst size becomes bigger. The viral lytic cycle may explain the oscillation phenomena observed in many studies. An important clinic implication is that the burst size should be carefully modified according to its effect on the lytic cycle when a type of a virus is modified for virotherapy, so that the period of the viral lytic cycle is in a suitable range which can break away the stability of the positive equilibria or periodic solutions.

1. Introduction

Oncolytic virotherapy is an innovative therapeutic strategy to destruct tumors. This idea stemmed from an old tale: evils can destroy evils. Viruses infect tumor cells and replicate themselves in tumor cells. Upon lysis of infected tumor cells, new virion particles burst out and proceed to infect additional tumor cells. This idea was initially tested in the middle of the last century, and merged with renewed interesting over last 20 years due to the technologic advances in virology and in the use of viruses as vectors for gene transfer. (For the history of oncolytic viruses, see [1].) Oncolytic viruses – viruses that selectively infect and replicate in tumor cells, but spare normal cells – have two types: oncolytic wild viruses that naturally occur with preferential in human cancer cells, and gene-modified viruses engineered to achieve selective oncolysis. The wild type viruses have shown a limited oncolytic efficacy in some preclinical trials, while gene-modified viruses seem to have a great potency of oncolysis [2–4]. The list of oncolytic viruses is growing (see [5] for a partial list). However, the efficacy of oncolytic

* Corresponding author.
E-mail address: weijj@hit.edu.cn (J. Wei).

0307-904X/$ - see front matter © 2012 Elsevier Inc. All rights reserved.
http://dx.doi.org/10.1016/j.apm.2012.12.004

virotherapy has not been well established yet. The major challenges are the replicative ability of oncolytic viruses within tumor cells and the spreadability of infections in whole tumors. Although genetic engineering has made possible to modify the viral genome to improve replicative ability of oncolytic viruses, the whole process of the lytic cycle of oncolytic viruses and viral infection spreading affects the outcome of oncolytic virotherapy. (For a review of oncolytic virotherapy, see [6].)

At molecular level, a great deal of the intracellular viral life cycle has been found out experimentally. The lytic cycle of a virus has six stages. To infect a cell, a virus must enter the cell through the plasma membrane. The virus attaches to a receptor on the cell membrane, and then releases its genetic materials into the cell. These are the first two stages, called adsorption and penetration. The third stage is integration that the host cell gene expression is arrested, and viral materials are embedded into the host cell nucleus. The fourth stage is biosynthesis that the virus uses the cell machinery to make large amount of viral components, and at the meantime, destroys the host's DNA. Then, it enters the last two stages, maturation and lysis. When many copies of viral components are made, they are assembled into complete viruses. The number of the newly formed viruses is call the *burst size* of the virus. These phages direct production of enzymes that break down the host cell membrane. The cell eventually bursts, and new viruses come out. (For the details of lytic cycle, see the book [7].) During the lytic cycle, each stage is mediated by a diverse group of proteins, and each stage needs some time to complete [8–11]. Overall, the burst size and the time period of the intracellular viral life cycle are important factors in viral therapy. Fig. 1 demonstrates the lytic cycle of oncolytic viruses.

At cell population level, many experiments have been conducted to test the outcome of oncolytic virotherapy. Some experiments with animal models have shown good results, and preclinical trials have achieved reasonable statistic results. All those research are still on phases I and II studies [12–15]. (For a review, see [5] and references therein.)

Oncolytic virotherapy, on the other hand, has provided opportunities for mathematical modeling. In return, mathematical models may help to understand this complicated treatment and to design efficient protocols. Actually, much effort has been devoted to mathematical studies on oncolytic virotherapy. Wu et al. [16,17] established a mathematical model in terms of partial differential equations (PDEs), which is essentially a radially-symmetric epidemic model with a freely moving boundary. They compared three alternative virus-injection strategies. Tao et al. proved there is a periodic solution for a similar PDE model as Wu's model [18]. We extended Wu's model to include innate immune responses and found the burst size is an important parameter for oncolytic virotherapy [19]. We also observed oscillation phenomena in our model. In order to thoroughly understand oncolytic virotherapy, it is better first to understand the dynamics of oncolytic virotherapy in a relative simple space-free setting. There are actually several works using ordinary differential equations (ODEs) to study the dynamics of oncolytic virotherapy. Wodarz proposed a mathematical model to study how virus-specific lytic CTL response contributes to killing of infected tumor cells [20]. Novozhilov et al. analyzed a ratio-dependent mathematical model for tumor cell population and infected tumor cell populations [21]. Bajzer et al. proposed a mathematical model for recombinant measles viruses. Their model counts free virus population besides tumor cell population and infected tumor cell populations [22]. Komarova et al. studied several possibilities to build mathematical models for oncolytic virus dynamics where only tumor cell population and infected tumor cell population are considered [23,24]. Based on Bajzer's model, we proposed a common basic mathematical model for oncolytic virotherapy with the parameter burst-size explicitly built in [25], and found the burst size is an important parameter for the dynamics of oncolytic treatments. However, all those mathematical models for oncolytic virotherapy do not consider the lytic cycle within infected tumor cells. To consider the intracellular viral life cycle, Tian et al. proposed a mathematical model [26], and found the viral life cycle can induce oscillations. However, this model does not count free virus population and the apoptosis blockade of infected tumor cells.

In this paper, we propose a mathematical model for the dynamics of oncolytic virotherapy with the viral lytic cycle incorporated. As mentioned above, the burst size and the time period of the intracellular viral life cycle are important factors in viral therapy. Theoretically, we will design two parameters b and τ to represent the burst size and the time period of the intracellular viral life cycle respectively, and assume these two parameters are constants. For simplicity, we will not model the details of the lytic cycle. Instead, we will use these two parameters to characterize the dynamics of viral therapy. Specifically, the population of infected tumor cells is determined by the populations of tumor cells and free viruses at τ unit time ago, and b new viruses add to free virus population once an infected tumor cell bursts. Such, the model is a nonlinear system of delay differential equations. Although the difficulty of analysis of the model, we obtain some analytical results. We also extend and confirm our analysis by numerical study of the model. One striking feature of the model is that the bifurcation value of the period of the viral lytic cycle is determined by the virus burst size. For the burst size, there are two threshold values. Below the first threshold, the system has an unstable trivial equilibrium and a globally stable viral free equilibrium. When the burst size is between two thresholds, the system has an asymptotically stable third interior equilibrium. When the burst size is above the second threshold, there is a functional relation between the bifurcation value of the delay parameter and the burst size. When the period of the lytic cycle is longer than the bifurcation value, the system undergoes Hopf bifurcation and has orbitally stable periodic solutions. However, this bifurcation value becomes smaller when the burst size becomes bigger. This prediction seems reasonable. When viruses have a big burst size, there will be more newly produced free viruses at unit time, and more infections at average. Then, it will need short time to accumulate enough infections to break away the stability of the co-exiting equilibrium for tumor cells, infected tumor cells and free viruses. This viral lytic cycle may explain the oscillation phenomena observed in many studies. An important clinic implication is that the burst size should be carefully modified according to its effect on the lytic cycle when a type of a virus is modified for virotherapy, so that the period of the viral lytic cycle is in a suitable range which can break away the stability of the interior equilibria or periodic solutions.

2. Mathematical models

In the paper [25], the basic mathematical model for oncolytic virotherapy was proposed as follows

$$\begin{cases} \frac{dx(t)}{dt} = \lambda x(t)(1 - \frac{x(t)+y(t)}{C}) - \beta x(t) v(t), \\ \frac{dy(t)}{dt} = \beta x(t) v(t) - \delta y(t), \\ \frac{dv(t)}{dt} = b\delta y(t) - \beta x(t) v(t) - \gamma v(t). \end{cases} \tag{2.1}$$

The variable x stands for the tumor cell population, y stands for the infected tumor cell population, and v represents free viruses which are outside cells. The tumor growth is modeled by logistic growth, and C is maximal tumor size, λ is the per capita tumor growth rate. The coefficient β represents the infectivity of the virus. The coefficient δ is the death rate of infected tumor cells, and γ is virus clearance rate. The parameter b is the burst size of the virus. For the details of the model assumptions, the reader is referred to the article [25].

As we mention in Introduction, this model and all other mathematical models do not incorporate lytic cycle within infected tumor cells. The time to complete the lytic cycle varies. For example, some virus only needs 30 min, some viruses take several hours to complete this process, and some can take days. Therefore, it is necessary and realistic to incorporate the lytic cycle into the oncolytic virotherapy model for its predicted dynamics. Moreover, to build a population model, we assume that the time period of the lytic cycle to be a constant τ. Based on the model (2.1), the rate of change of infected tumor cells at time t will be determined by the tumor cell population and free virus at time $t - \tau$, namely, $x(t - \tau)v(t - \tau)$. Although the details of the lytic cycle as shown in Fig. 1 will not be incorporated into the model, we will use the lytic cycle time τ and burst size to catch the oncolytic process. Based on the model (2.1), a diagram for the dynamic interactions in oncolytic virotherapy within a tumor is given in Fig. 2.

Because of the apoptosis blockade of infected tumor cells [5], infected tumor cells will not die until they burst. That is, a death term for infected tumor cells before bursting is not necessary, and all infected tumor cells will burst. Therefore, the model we propose is given by the system (2.2).

$$\begin{cases} \frac{dx(t)}{dt} = \lambda x(t)(1 - \frac{x(t)+y(t)}{C}) - \beta x(t) v(t), \\ \frac{dy(t)}{dt} = \beta x(t - \tau) v(t - \tau) - \delta y(t), \\ \frac{dv(t)}{dt} = b\delta y(t) - \beta x(t) v(t) - \gamma v(t). \end{cases} \tag{2.2}$$

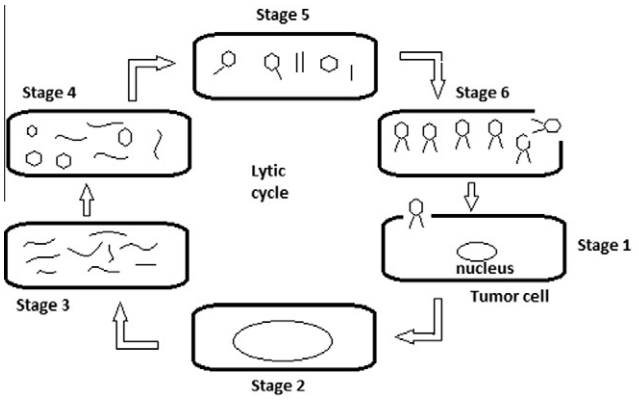

Fig. 1. The lytic cycle of oncolytic viruses.

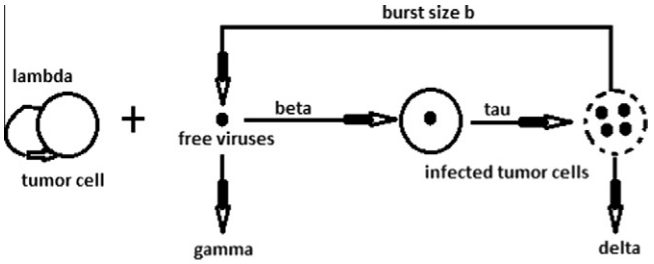

Fig. 2. The interactions in oncolytic virotherapy. λ is per capita growth rate. β is infectivity. τ is the period of time of lytic cycle. γ is virus clearance rate. δ is death of infected tumor cells.

For the convenience of study, we re-scale this system by setting $\tilde{t} = \delta t,\ \tilde{\tau} = \delta\tau,\ x(t) = C\tilde{x}(\tilde{t}),\ y(t) = C\tilde{y}(\tilde{t}),$ and $v(t) = C\tilde{v}(\tilde{t})$. Then, we drop all tildes over variables. The non-dimensionalized system is given by (2.3).

$$\begin{cases} \frac{dx(t)}{dt} = k_1 x(t)(1 - x(t) - y(t)) - k_2 x(t) v(t), \\ \frac{dy(t)}{dt} = k_2 x(t-\tau) v(t-\tau) - y(t), \\ \frac{dv(t)}{dt} = b y(t) - k_2 x(t) v(t) - k_3 v(t), \end{cases} \tag{2.3}$$

where $k_1 = \frac{\lambda}{\delta},\ k_2 = \frac{C\beta}{\delta},\ k_3 = \frac{\gamma}{\delta}$.

3. Preliminary results

To study the dynamics of the system (2.3) when $\tau \geqslant 0$, we need to consider a suitable phase space and a feasible region. For $\tau > 0$, let $\mathcal{C} = C([-\tau, 0], \mathbb{R})$ be the Banach space of continuous functions mapping the interval $[-\tau, 0]$ into $\mathbb{R}$ with the norm $\|\varphi(\theta)\| = sup_{-\tau\leqslant\theta\leqslant 0}|\varphi(\theta)|$ for $\varphi \in \mathcal{C}$. The nonnegative cone of $\mathcal{C}$ is denoted by $\mathcal{C}^+ = C([-\tau, 0], \mathbb{R}_+)$. We present some preliminary results for the system (2.3). Particularly, when the burst size b is smaller than the first threshold $b_{c_1} = 1 + \frac{k_3}{k_2}$, the virotherapy fails no matter what the lytic cycle period is.

Proposition 3.1. *Suppose that $(x(t), y(t), v(t))$ is a solution of system (2.3) with initial conditions $x(\theta) = \varphi_1(\theta),\ y(\theta) = \varphi_2(\theta)$, and $v(\theta) = \varphi_3(\theta)$, where $\varphi_i(\theta) \in \mathcal{C}^+$, and $\varphi_i(0) > 0,\ i = 1, 2, 3$. Then $x(t) \geqslant 0,\ y(t) \geqslant 0,\ v(t) \geqslant 0$ for all $t \geqslant 0$.*

Proof. From the first equation of the system (2.3) we have that

$$x(t) = \varphi_1(0) e^{\int_0^t [k_1(1 - x(s) + y(s)) - k_2 v(s)] ds}.$$

Since $\varphi_1(0) \geqslant 0$, it implies that $x(t) \geqslant 0$ for $t \geqslant 0$.

When $t \in [0, \tau]$, from the second equation of system (2.3) it follows that

$$y(t) = e^{-t}\left[\varphi_2(0) + k_2 \int_0^t e^s \varphi_1(s - \tau)\varphi_3(s - \tau) ds\right].$$

Since $\varphi_i(\theta) \geqslant 0$ $(i = 1, 2, 3)$, we have $y(t) \geqslant 0$ when $t \in [0, \tau]$.

From the third equation of system (2.3) we have that

$$v(t) = e^{-\int_0^t (k_3 + k_2 x(s)) ds}\left[\varphi_3(0) + b \int_0^t e^{\int_0^s (k_3 + k_2 x(\xi)) d\xi} y(s) ds\right]$$

and $\varphi_3(0) \geqslant 0$, as well as $y(t) \geqslant 0$ for $t \in [0, \tau]$, we have $v(t) \geqslant 0$ for $t \in [0, \tau]$.

By induction, we have that $y(t) \geqslant 0$ and $v(t) \geqslant 0$ for all $t \geqslant 0$. Hence the proof is completed. □

Proposition 3.2. *For the initial conditions in Proposition 3.1, the solutions of system (2.3) are ultimately uniformly bounded in $\mathcal{C}^+ \times \mathcal{C}^+ \times \mathcal{C}^+$ for $t \geqslant 0$.*

Proof. By Proposition 3.1, we have that $\frac{d}{dt}x(t) \leqslant k_1 x(t) - k_1 x^2(t)$. By the Comparison Principle, we can get $x(t) \leqslant 1$ when the initial value $x(0) < 1$. Therefore, $\limsup_{t\to+\infty} x(t) \leqslant 1$. Furthermore, we consider

$$\begin{aligned} (x(t-\tau) + y(t))' &= k_1 x(t-\tau)[1 - x(t-\tau) - y(t-\tau)] - y(t) \\ &\leqslant k_1[1 - x(t-\tau)] - y(t) \\ &= k_1 - k_1 x(t-\tau) - y(t) \end{aligned}$$

with $0 \leqslant \varphi_1 \leqslant 1,\ 0 \leqslant \varphi_2 \leqslant \frac{k_1}{k}$ and $k = \min\{k_1, 1\}$. We obtain $\limsup_{t\to+\infty}[x(t-\tau) + y(t)] \leqslant \frac{k_1}{k}$. Since $x(t) \geqslant 0$, we get $\limsup_{t\to+\infty} y(t) \leqslant \frac{k_1}{k}$. The third equation of system (2.3) implies

$$v'(t) = b y(t) - k_2 x(t) v(t) - k_3 v(t) \leqslant b y(t) - k_3 v(t) \leqslant b\frac{k_1}{k} - k_3 v(t),$$

thus, $\limsup_{t\to+\infty} v(t) \leqslant \frac{bk_1}{kk_3}$. Therefore, $x(t),\ y(t)$, and $v(t)$ are ultimately uniformly bounded in $\mathcal{C}^+ \times \mathcal{C}^+ \times \mathcal{C}^+$. □

Proposition 3.2 implies that the ω limit set of system (2.3) is contained in the following bounded feasible region:

$$M = \left\{(x, y, v) \in \mathcal{C}^+ \times \mathcal{C}^+ \times \mathcal{C}^+ : \|x\| \leqslant 1, \|y\| \leqslant \frac{k_1}{k}, \|v\| \leqslant \frac{bk_1}{kk_3}\right\}.$$

It is easy to verify that the region M is positively invariant for the system (2.3). We will analyze the model in this region.

When $b \leqslant b_{c_1} = 1 + \frac{k_3}{k_2}$, the system has two equilibria $E_0 = (0, 0, 0)$, and $E_1 = (1, 0, 0)$. The E_0 is cancer free equilibrium, and E_1 is infection free but with cancer equilibrium. When $b > b_{c_1}$, there is a third equilibrium $E^* = (x^*, y^*, v^*)$ in the feasible range, where

$$x^* = \frac{k_3}{k_2(b-1)}, \quad y^* = \frac{k_3}{b-1}v^*, \quad v^* = \frac{k_1k_2(b-1)-k_1k_3}{k_2(k_1k_3+k_2(b-1))}.$$

If the burst size b is less than 1, then free viruses will die out eventually. It is impossible to establish any infection within a tumor in this situation. Actually, the burst size is even greater than 1 but smaller than $b_{c_1} = 1 + \frac{k_3}{k_2}$, it is still impossible for virus infection spreading. At the cancer free and hence virus free equilibrium $E_0 = (0,0,0)$, the eigenvalues of variational matrix of the system (2.3) are

$$\mu_1 = k_1 > 0, \quad \mu_2 = -1 < 0, \quad \mu_3 = -k_3 < 0.$$

Therefore, this equilibrium is unstable for biologically relevant parameters. Biologically, around the origin, each population has a small size, virus population and infected tumor cell population both decrease, but tumor cell population increases. The instability of this equilibrium is due to the increase of tumor cells. Furthermore, as the tumor population attains its maximal size 1, the equilibrium $E_1 = (1,0,0)$ represents failure of the tumor virotherapy.

Proposition 3.3. *The equilibrium E_1 is locally asymptotically stable for any time delay $\tau \geqslant 0$ if $b < b_{c_1}$, and unstable if $b > b_{c_1}$.*

Proof. Let $u_1 = x - 1,\ u_2 = y$, and $u_3 = v$, the system (2.3) is transformed as

$$\begin{cases} \frac{du_1(t)}{dt} = -k_1u_1(t) - k_1u_2(t) - k_2u_3(t) - k_1u_1^2(t) - k_1u_1(t)u_2(t) - k_2u_1(t)u_3(t), \\ \frac{du_2(t)}{dt} = -u_2(t) + k_2u_3(t-\tau) + k_2u_1(t-\tau)u_3(t-\tau), \\ \frac{du_3(t)}{dt} = bu_2(t) - (k_2+k_3)u_3(t) - k_2u_1(t)u_3(t). \end{cases} \tag{3.1}$$

Then the characteristic equation is

$$(\mu + k_1)[(\mu+1)(\mu+k_2+k_3) - bk_2e^{-\mu\tau}] = 0. \tag{3.2}$$

Clearly, $\mu = -k_1$ is a root of the Eq. (3.2). So we only need to consider

$$\mu^2 + a_1\mu + b_1 + c_1e^{-\mu\tau} = 0, \tag{3.3}$$

where $a_1 = 1 + k_2 + k_3 > 0$, $b_1 = k_2 + k_3 > 0$, $c_1 = -bk_2$.

$b < 1 + \frac{k_3}{k_2}$ implies that $b_1 + c_1 = k_2 + k_3 - bk_2 > 0$. Hence, the roots of (3.3) at $\tau = 0$ have negative real parts. This shows that the equilibrium E_1 is locally asymptotically stable when $\tau = 0$.

$i\omega(\omega > 0)$ is a root of (3.3) with $\tau > 0$ if and only if

$$-\omega^2 + ia_1\omega + b_1 + c_1(\cos\omega\tau - i\sin\omega\tau) = 0.$$

Separating the real and imaginary parts gives

$$\begin{cases} -\omega^2 + b_1 = -c_1\cos\omega\tau, \\ -a_1\omega = -c_1\sin\omega\tau. \end{cases} \tag{3.4}$$

Adding the squares of both equations together, we obtain

$$\omega^4 + (a_1^2 - 2b_1)\omega^2 + b_1^2 - c_1^2 = 0. \tag{3.5}$$

Then

$$\omega^2 = \frac{1}{2}\left[-(a_1^2 - 2b_1) \pm \sqrt{(a_1^2-2b_1)^2 - 4(b_1^2 - c_1^2)}\right].$$

This implies that $\omega^2 < 0$ when $b < 1 + \frac{k_3}{k_2}$. Hence, all the roots of (3.3) have negative real parts when $b < 1 + \frac{k_3}{k_2}$. Thus, the equilibrium E_1 is locally asymptotically stable for any time delay $\tau \geqslant 0$. Let

$$h(\mu) = \mu^2 + a_1\mu + b_1 + c_1e^{-\mu\tau}.$$

Then we have $\lim_{\mu\to+\infty} h(\mu) = +\infty$ and $h(0) = b_1 + c_1 < 0$ when $b > 1 + \frac{k_3}{k_2}$. It follows that the equation $h(\mu) = 0$ has at least one positive root. Hence E_1 is unstable for $\tau \geqslant 0$. □

Theorem 3.4. *If $b < b_{c_1}$, the equilibrium E_1 is globally asymptotically stable for all $\tau \geqslant 0$.*

Proof. Consider a Lyapunov functional on the domain M given by

$$V(\phi) = b\varphi_2(0) + \varphi_3(0) + bk_2\int_{-\tau}^{0}\varphi_1(s)\varphi_3(s)ds.$$

When $b < 1 + \frac{k_3}{k_2}$, we have

$$\dot{V}(\phi) = [k_2\varphi_1(0)(b-1) - k_3]\varphi_3(0) \leqslant [k_2(b-1) - k_3]\varphi_3(0) \leqslant 0.$$

Meanwhile, we have $\dot{V}(\phi) = 0$ if and only if $\varphi_3(0) = 0$. Thus, the maximum invariant set in $\{\phi \in M | \dot{V}(\phi) = 0\}$ is the singleton E_1. The classical Lasalle's Invariance Principle [27] implies that $E_1 = (1, 0, 0)$ is globally attractive. This confirms the globally asymptotical stability of E_1 for $\tau \geqslant 0$. □

4. Hopf bifurcations and periodic solutions

When the burst size b is greater than the first threshold b_{c_1}, the system (2.3) has the third interior equilibrium E^*. There exists the second threshold of the burst size, b_{c_2} which is greater than b_{c_1}. When the burst size b is greater than b_{c_2}, there exists bifurcation value for the lytic cycle period τ_0. When $0 \leqslant \tau \leqslant \tau_0$, E^* is locally asymptotically stable. While the system undergoes Hopf bifurcation at $\tau = \tau_0$. When the lytic cycle period is greater than τ_0, there exists periodic solutions. To study periodic solutions, we compute the directions of Hopf bifurcations, the Floquet exponents of the periodic solutions and their periods. However, we leave the theoretical derivation in Appendix A.

4.1. Existence of Hopf bifurcations and periodic solutions

By the transformation $u_1 = x - x^*$, $u_2 = y - y^*$, $u_3 = v - v^*$, the system (2.3) is changed to

$$\begin{cases} \frac{du_1}{dt} = -k_1x^*u_1(t) - k_1x^*u_2(t) - k_2x^*u_3(t) - k_1u_1^2(t) - k_1u_1(t)u_2(t) - k_2u_1(t)u_3(t), \\ \frac{du_2}{dt} = -u_2(t) + k_2v^*u_1(t-\tau) + k_2x^*u_3(t-\tau) + k_2u_1(t-\tau)u_3(t-\tau), \\ \frac{du_3}{dt} = -k_2v^*u_1(t) + bu_2(t) - (k_2x^* + k_3)u_3(t) - k_2u_1(t)u_3(t). \end{cases} \tag{4.1}$$

The linearization of (4.1) at $(0, 0, 0)$ is given by

$$\begin{cases} \frac{du_1}{dt} = -k_1x^*u_1(t) - k_1x^*u_2(t) - k_2x^*u_3(t), \\ \frac{du_2}{dt} = -u_2(t) + k_2v^*u_1(t-\tau) + k_2x^*u_3(t-\tau), \\ \frac{du_3}{dt} = -k_2v^*u_1(t) + bu_2(t) - (k_2x^* + k_3)u_3(t). \end{cases} \tag{4.2}$$

Then the characteristic equation is

$$\mu^3 + a_1\mu^2 + b_1\mu + c_1 + (d_1\mu + e_1)e^{-\mu\tau} = 0, \tag{4.3}$$

where

$$a_1 = k_3 + k_2x^* + 1 + k_1x^*,$$

$$b_1 = k_3 + k_1k_3x^* + k_2x^* + k_1k_2x^{*2} + k_1x^* - k_2^2x^*v^*,$$

$$c_1 = k_1x^*(k_3 + k_2x^*) - k_2^2x^*v^*,$$

$$d_1 = k_1k_2x^*v^* - bk_2x^*,$$

$$e_1 = bk_2^2x^*v^* - bk_1k_2x^{*2} + k_1k_2k_3x^*v^*.$$

It is impossible to find roots of the Eq. (4.3) explicitly. Instead, we look for the condition under which it has purely imaginary roots and there will be Hopf bifurcations. Particularly, we are interested in the condition that relates the burst size b and the delay parameter τ. Clearly, $i\omega(\omega > 0)$ is a root of (4.3) if and only if

$$-i\omega^3 - a_1\omega^2 + ib_1\omega + c_1 + (id_1\omega + e_1)(\cos\omega\tau - i\sin\omega\tau) = 0.$$

Separating the real and imaginary parts, we have

$$\begin{cases} -a_1\omega^2 + c_1 = -d_1\omega\sin\omega\tau - e_1\cos\omega\tau, \\ -\omega^3 + b_1\omega = -d_1\omega\cos\omega\tau + e_1\sin\omega\tau. \end{cases}$$

Adding the squares of both equations together gives

$$\omega^6 + (a_1^2 - 2b_1)\omega^4 + (b_1^2 - 2a_1c_1 - d_1^2)\omega^2 + c_1^2 - e_1^2 = 0. \tag{4.4}$$

Denote $z = \omega^2$, $p = a_1^2 - 2b_1$, $q = b_1^2 - 2a_1c_1 - d_1^2$ and $r = c_1^2 - e_1^2$. Then the Eq. (4.4) becomes

$$h(z) = z^3 + pz^2 + qz + r = 0. \tag{4.5}$$

Suppose the Eq. (4.5) has positive roots. Without loss of generality, we assume that it has three positive roots, denoted by z_1, z_2 and z_3, respectively. Then the Eq. (4.4) has three positive roots, say

$$\omega_1 = \sqrt{z_1}, \quad \omega_2 = \sqrt{z_2}, \quad \omega_3 = \sqrt{z_3}.$$

Let

$$\tau_k^{(j)} = \frac{1}{\omega_k}\left\{\arccos\left[\frac{d_1\omega_k^4 + (a_1e_1 - b_1d_1)\omega_k^2 - c_1e_1}{d_1^2\omega_k^2 + e_1^2}\right] + 2j\pi\right\}, \quad k = 1,2,3,\ j = 1,2,\ldots \tag{4.6}$$

Then $\pm i\omega_k$ is a pair of purely imaginary roots of (4.3) with $\tau = \tau_k^{(j)},\ k = 1,2,3,\ \ j = 1,2,\ldots$ Clearly, $\lim_{j\to\infty}\tau_k^{(j)} = \infty,\ k = 1,2,3, j \geqslant 1$. Then we can define

$$\tau_0 = \tau_{k_0}^{(j_0)} = \min_{1 \leqslant k \leqslant 3, j \geqslant 1}\{\tau_k^{(j)}\}, \quad \omega_0 = \omega_{k_0}. \tag{4.7}$$

When $\tau = 0$, the Eq. (4.3) becomes

$$\mu^3 + a_1\mu^2 + b_1\mu + c_1 + d_1\mu + e_1 = 0. \tag{4.8}$$

By the Routh–Hurwitz criterion, all of its roots have negative real parts if and only if $a_1 > 0,\ a_1(b_1 + d_1) - (c_1 + e_1) > 0$ *and* $c_1 + e_1 > 0$. When $b > b_{c_1},\ a_1 > 0$, and

$$\begin{aligned} c_1 + e_1 &= k_1x^*(k_3 + k_2x^*) - k_2^2x^*v^* + bk_2^2x^*v^* - bk_1k_2x^{*2} + k_1k_2k_3x^*v^* \\ &= (1-b)k_1k_2x^{*2} + k_1k_3x^* + (b-1)k_2^2x^*v^* + k_1k_2k_3x^*v^* = (b-1)k_2^2x^*v^* + k_1k_2k_3x^*v^* > 0. \end{aligned}$$

If $a_1(b_1 + d_1) - (c_1 + e_1) > 0$, then

$$a_1(b_1 + d_1) > (c_1 + e_1),$$

$$(k_3 + k_2x^* + 1 + k_1x^*)(k_3 + k_1k_3x^* + k_2x^* + k_1k_2x^{*2} + k_1x^* - k_2^2x^*v^* + k_1k_2x^*v^* - bk_2x^*) > ((b-1)k_2^2x^*v^* + k_1k_2k_3x^*v^*),$$

$$(k_3 + k_2x^* + 1 + k_1x^*)(k_1k_3 + k_1k_2x^* + k_1 - k_2^2v^* + k_1k_2v^*) > ((b-1)k_2^2v^* + k_1k_2k_3v^*),$$

$$k_1k_3 + k_1k_2x^* + k_1 - k_2^2v^* + k_1k_2v^* > \frac{(b-1)k_2^2v^* + k_1k_2k_3v^*}{k_3 + k_2x^* + 1 + k_1x^*},$$

$$\frac{k_1k_3b + k_1(b-1)}{b-1} + \frac{(k_1 - k_2)(k_1k_2(b-1) - k_1k_3)}{k_1k_3 + k_2(b-1)} > \frac{(k_1k_2(b-1) - k_1k_3)k_2(b-1)}{(k_2k_3b + k_2(b-1) + k_1k_3)},$$

$$\frac{(k_3b + b - 1)(k_1k_3 + k_2(b-1))}{(k_2(b-1) - k_3)(b-1)} + k_1 - k_2 > \frac{k_2(b-1)((b-1)k_2 + k_1k_3)}{k_2k_3b + k_2(b-1) + k_1k_3},$$

$$\frac{k_2(b-1)}{k_2k_3b + k_2(b-1) + k_1k_3} - \frac{k_3b + b - 1}{(k_2(b-1) - k_3)(b-1)} < \frac{k_1 - k_2}{k_1k_3 + k_2(b-1)}.$$

Since $k_1k_3 + k_2(b-1) > 0$, we obtain $\phi(b) < k_1 - k_3$. From the derivation above, we see that $a_1(b_1 + d_1) - (c_1 + e_1) > 0$ if and only if $\phi(b) < k_1 - k_3$. Therefore, we conclude that all roots of the Eq. (4.8) have negative real parts if and only if $\phi(b) < k_1 - k_3$ when $b > b_{c_1}$. To summary, we quote a statement from [28].

Lemma 4.1 (*see [28]*). *Suppose that* $b > b_{c_1}$ *and* $\phi(b) < k_1 - k_3$. *Then*

(i) *If* $r \geqslant 0$ *and* $\triangle = p^2 - 3q < 0$, *then all roots of the Eq. (4.3) have negative real parts for all* $\tau \geqslant 0$
(ii) *If* $r < 0$ *or* $r \geqslant 0,\ z_1 > 0$ *and* $h(z_1) \leqslant 0$, *then all roots of the Eq. (4.3) have negative real parts when* $\tau \in [0, \tau_0)$.

Consider $r = c_1^2 - e_1^2 = (c_1 + e_1)(c_1 - e_1)$.

$$\begin{aligned} c_1 - e_1 &= k_1k_3x^* + k_1k_2(b+1)x^{*2} - (k_2^2 + bk_2^2 + k_1k_2k_3)x^*v^* = x^*[k_1k_3 + k_1k_2(b+1)x^* - (k_2^2 + bk_2^2 + k_1k_2k_3)v^*] \\ &= x^*k_1\left[k_3 + \frac{k_3(b+1)}{b-1} - (k_2 + bk_2 + k_1k_3)\frac{k_2(b-1) - k_3}{k_1k_3 + k_2(b-1)}\right] \\ &= x^*k_1\left[k_3 + \frac{k_3(b+1)}{b-1} - \frac{k_1k_3 + k_2(b+1)}{k_1k_3 + k_2(b-1)}(k_2(b-1) - k_3)\right] \\ &= x^*k_1\left[\frac{2bk_3(b+1)}{b-1} - \frac{k_1k_3 + k_2(b+1)}{k_1k_3 + k_2(b-1)}(k_2(b-1) - k_3)\right]. \end{aligned}$$

Since $x^*k_1 > 0$, setting $b - 1 = y$, we only consider the factor Ψ

$$\Psi = \frac{2(1+y)k_3}{y} - \frac{k_1k_3 + k_2(2+y)}{k_1k_3 + k_2y}(k_2y - k_3) = \frac{\psi(y)}{y(k_1k_3 + k_2y)},$$

where $\psi(y) = -k_2^2y^3 - (k_1k_2k_3 + 2k_2^2 - 3k_2k_3)y^2 + (3k_1k_3^2 + 4k_2k_3)y + 2k_1k_3^2$. Ψ and $\psi(y)$ have the same nonzero roots. We only need to study the root distribution of $\psi(y)$.

Consider $\psi'(y) = -3k_2^2y^2 - 2(k_1k_2k_3 + 2k_2^2 - 3k_2k_3)y + 4k_2k_3$. Since $4k_2k_3 > 0$, $\psi'(y)$ has two roots, and with opposite signs. Say $y_1 < 0,\ y_2 > 0$. Since $\psi(0) = 2k_1k_3^2 > 0,\ \psi(y) \to +\infty$ as $y \to -\infty$, and $\phi(y) \to -\infty$ as $y \to +\infty$, so $\psi(y_1) < 0$ and $\phi(y_2) > 0$, there is a root y_3 of $\psi(y) = 0$ such that $\psi(y) < 0$ when $y > y_3$, while $\psi(y) > 0$ when $0 < y < y_3$. Since $\psi(\frac{k_3}{k_2}) > 0$, so $y_3 > \frac{k_3}{k_2}$. Denote $b_{c_2} = 1 + y_3$, then $b_{c_2} > b_{c_1}$. Therefore, when $b > b_{c_2},\ r = (c_1 + e_1)(c_1 - e_1) < 0$.

Lemma 4.2. *If $\phi(b) < k_1 - k_3$ and $b > b_{c_2}$, there exists a positive value τ_0, such that all roots of the Eq. (4.3) have negative real parts when $\tau \in [0, \tau_0)$.*

Let

$$\mu(\tau) = \alpha(\tau) + i\omega(\tau)$$

be the root of the Eq. (4.3) satisfying $\alpha(\tau_0) = 0$ and $\omega(\tau_0) = \omega_0,\ z_0 = \omega_0^2$. It needs to be confirmed if $\pm i\omega_0$ is a pair of simple purely imaginary roots. We need to verify $h'(z_0) \neq 0$.

Consider the coefficient p of the Eq. (4.5), $p = a_1^2 - 2b_1 = (k_1^2 + k_2^2)x^{*2} + 2k_2k_3x^* + k_2^2x^*v^* + k_3^2 + 1 > 0$. Suppose z_0 is a repeated root, then z_0 is also a root of $h'(z) = 0$. The roots of $h'(z) = 3z^2 + 2pz + q = 0$ are given by $z_1 = -\frac{p}{3} + \frac{1}{3}\sqrt{p^2 - 3q}$ and $z_2 = -\frac{p}{3} - \frac{1}{3}\sqrt{p^2 - 3q}$, which both are real. Since $p > 0,\ z_2$ is negative. So, z_0 must be z_1. Such, we have $(z - z_0)(z - z_1)(z - z_2) = (z - z_1)(z - z_1)(z - z_2) = z^3 + pz^2 + qz + r$. Compare their coefficients, we have $z_1^2z_2 = -r > 0$ since r is negative when $b > b_{c_2}$. However, $z_1^2z_2 < 0$. This contradiction means z_0 is not a repeated root. Therefore, $h'(z_0) \neq 0$.

We also need to know the sign of $\alpha'(\tau)$ at $\tau = \tau_0$, which will tell monotonicity of the function $\alpha(\tau)$ around τ_0. We differentiate both sides of the Eq. (4.3) with respect to τ, and obtain

$$\{3\mu^2 + 2a_1\mu + b_1 + [d_1 - \tau(d_1\mu + e_1)]e^{-\mu\tau}\}\frac{d\mu}{d\tau} = \mu(d_1\mu + e_1)e^{-\mu\tau}.$$

Solving for the derivative, we have

$$\left(\frac{d\mu}{d\tau}\right)^{-1} = \frac{(3\mu^2 + 2a_1\mu) + b_1)e^{\mu\tau}}{\mu(d_1\mu + e_1)} + \frac{d_1 - \tau(d_1\mu + e_1)}{\mu(d_1\mu + e_1)}.$$

Therefore,

$$Sign\frac{dRe\mu(\tau_0)}{d\tau} = Sign\left\{Re\left(\frac{d\mu}{d\tau}\right)^{-1}|_{\tau=\tau_0}\right\} = Sign\left\{\frac{1}{d_1^2\omega_0^2 + e_1^2}h'(z_0)\right\} \neq 0.$$

We state the results above as a Theorem 4.3

Theorem 4.3. *If $\phi(b) < k_1 - k_3$ and $b > b_{c_2}$, there exists a positive value τ_0, such that all roots of the Eq. (4.3) have negative real parts when $\tau \in [0, \tau_0)$. While at $\tau = \tau_0$, the Eq. 4.3 has a pair of simple purely imaginary roots, $\pm i\omega_0$, and all other roots have negative real parts. Furthermore,*

$$Sign\left\{\frac{d\alpha(\tau_0)}{d\tau}\right\} = Sign\{h'(z_0)\}.$$

4.2. Numerical study of Hopf bifurcations and periodic solutions

To demonstrate the model behavior, we simulate the system (2.3). According to data in [19], we choose a set of parameter values as follows: $k_1 = 0.1,\ k_2 = 0.001,\ k_3 = 0.01$. Since we are interested in how the burst size b and the period of the lytic cycle τ influence the virotherapy, we will leave these two parameters as variables. The thresholds of the burst size are determined by other three parameters. We compute $b_{c_1} = 1 + \frac{k_3}{k_2} = 11$. To compute b_{c_2}, we solve the equation $\psi(y) = 0$ to find the positive root (it has only one positive root) y_3, and b_{c_2} is given by $b_{c_2} = 1 + y_3 \approx 30$. We know that $p > 0$ and $r < 0$ if $b > b_{c_2}$ in the Eq. (4.5). Then, the Eq. (4.5) has only one positive root. So, the Hopf bifurcation value τ_0 is easy to define and compute in terms of the burst size b as (4.6). We plot the relation between τ_0 and b when $b > b_{c_2}$ in Fig. 3. It is easy to observe that τ_0 is a decreasing function of b. That means, when the virus burst size is big, the time for the virotherapy to get out the stability of the interior equilibrium is short, and the system may shift to oscillated interaction among three populations.

We take several typical cases to demonstrate the what may happen for the system. When $b = 100$, we compute $\tau_0(100) = 13.99$. If we take $\tau = 9$, the equilibrium E^* should be asymptotically stable. The Fig. 4 shows this situation.

For $b = 100$ and $\tau_0(100) = 13.99$, if we take $\tau = 16$, we obtain periodic solutions for different initial conditions. Fig. 5 show oscillation of each population over time and oscillated interactions between three populations.

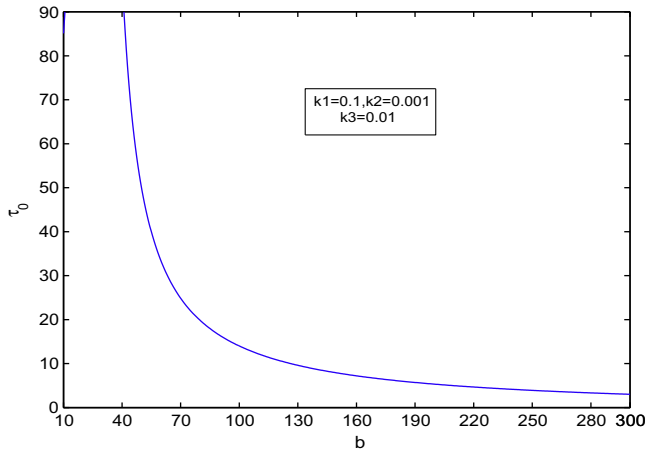

Fig. 3. A bifurcation curve $\tau_0(b)$: for a fixed value of the burst size b, there corresponds to a value of the lytic cycle period τ_0 according to the curve. The system undergoes a Hopf bifurcation when τ passes τ_0.

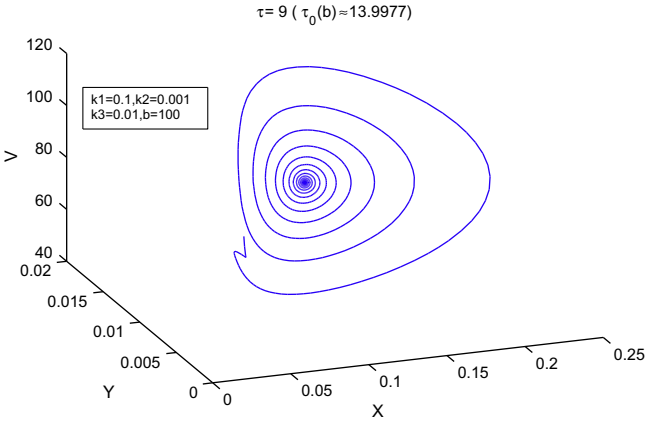

Fig. 4. The initials are $x(0) = 0.025,\ y(0) = 0.0001$, and $v(0) = 85$. The equilibrium components are $x^* = 0.1,\ y^* = 0.009$, and $v^* = 90$.

To Study these periodic solutions, we study the directions of bifurcations, the Floquet exponents and periods of bifurcating solutions. The theoretical derivation is given in Appendix A. We compute $c_1(0) = -0.0238 - 0.4238i$, hence $Re\{c_1(0)\} < 0$. We also get $Re\{\mu'(\tau_0)\} > 0,\ \mu_2 > 0,\ \beta_2 = -0.0476 < 0$. Therefore, the positive equilibrium E^* is asymptotically stable when $\tau \in [0, 13.99)$, the Hopf bifurcation is supercritical and the bifurcating periodic solution is orbitally stable when $\tau > \tau_0$.

We know from the function $\psi(b)$ that the system will not undergo Hopf bifurcations around E^* when the value of b choose as $b_{c_1} = 11 < b < b_{c_2} = 30$.

On the other hand, we choose the burst size b as a bifurcating parameter. We fix the lytic cycle period, say $\tau = 8$, according to the relation between τ_0 and b as shown in Fig. 3, we obtain $b^* \approx 133$. To demonstrate, we take two different values of the burst size, $b = 100$ and $b = 150$. Fig. 6 shows the positive equilibrium E^* is asymptotically stable.

When the burst size $b = 150 > 133$, we have periodic solutions for different initial conditions. Fig. 7 shows the dynamics of each population over time and interactions among them. We also did computation in Appendix A, and find these Hopf bifurcations are supercritical and the bifurcating periodic solutions are orbitally stable.

In summary, when the burst size b and the lytic cycle τ are above the bifurcation curve in Fig. 3, the system has periodic solutions. When b and τ are below the bifurcation curve and $b > b_{c_2}$, the system has the stable interior equilibrium solution. Along the bifurcation curve, the system undergoes Hopf bifurcations.

5. Summary and discussion

The viral lytic cycle is the most important process in oncolytic virotherapy. After the initial infection of tumor cells by oncolytic viruses, new viruses are produced by this virus reproduction process. It makes the spreading of the infection within a tumor possible. It is clear that any initial infection of tumor cells by injecting viruses can not have a successful experimen-

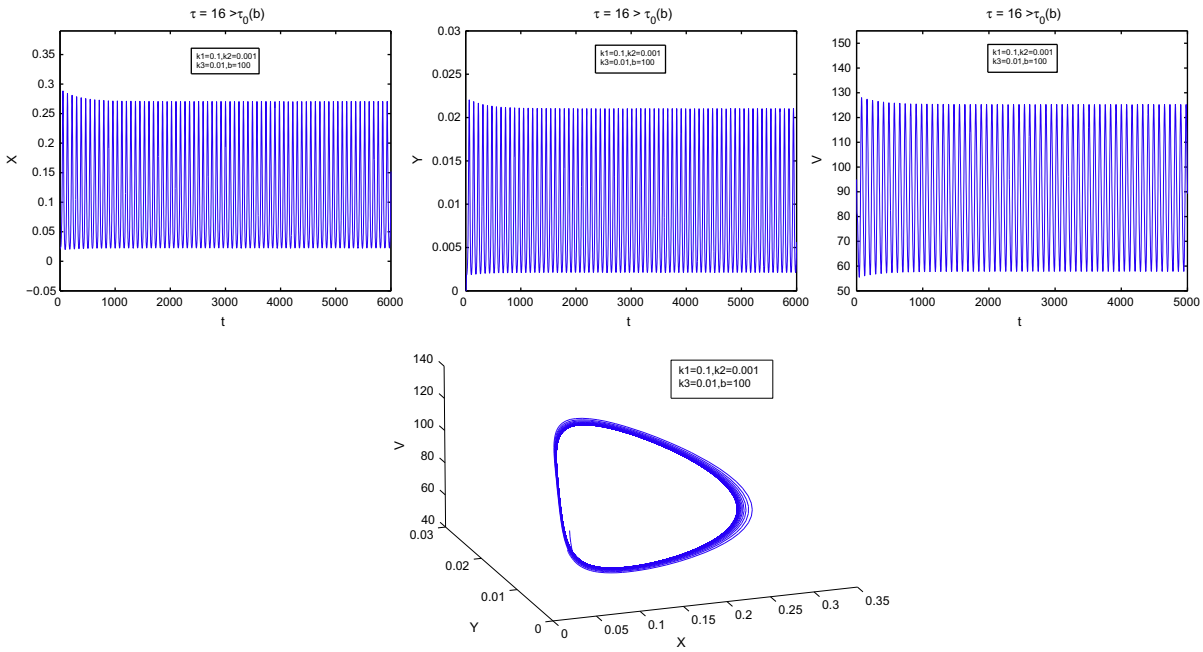

Fig. 5. Periodic solutions when $\tau > \tau_0$.

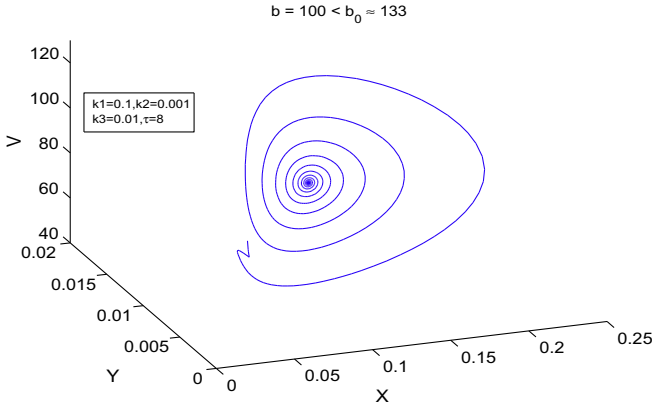

Fig. 6. The initials are $x(0) = 0.025,\ y(0) = 0.0001$, and $v(0) = 85$. The equilibrium components are $x^* = 0.1,\ y^* = 0.009$, and $v^* = 90$.

tal or clinical results, and even cannot establish a meaningful infection. Therefore, the understanding of the viral lytic cycle within a tumor is essential for improving experimental and clinical efficacy of virotherapy.

The dynamics of the viral lytic cycle can be described by two parameters, the viral burst size and the time period of the viral lytic cycle. In this article, we study the viral lytic cycle by applying delayed differential equations. The model is a nonlinear system of three differential equations. It explicitly incorporates the burst size b and the period of the viral lytic cycle τ. The dynamic behavior of the model is characterized by those two parameters. Particularly, the burst size has two threshold values, b_{c_1} and b_{c_2}. The model always has two equilibrium solutions, the trivial one E_0 and the virus free equilibrium solution E_1 while it has the third positive equilibrium solution E^* when $b > b_{c_1}$. E_0 is always unstable. By employing a Lyapunov functional, it is shown E_1 is globally asymptotically stable for any lytic cycle period $\tau \geqslant 0$ when $b < b_{c_1}$, while it is unstable when $b > b_{c_1}$. When the burst size b is greater than the second threshold b_{c_2}, there exists a bifurcation value for the lytic cycle period τ_0. For this b, if $\tau < \tau_0$, the positive equilibrium solution E^* is locally asymptotically stable. The system undergoes a Hopf bifurcation around $\tau = \tau_0$. When $\tau > \tau_0$, the system has orbitally stable periodic solutions. It is interesting that τ_0 is a function of b when $b > b_{c_2}$. The system also undergoes a Hopf bifurcation along the parameter b. Therefore, we obtain a bifurcation curve in $b - \tau$ plane. The system undergoes Hopf bifurcations along this curve. For the values of b and τ that are above this curve, the system has periodic solutions. For the values of b and τ that are below this curve, the system has stable

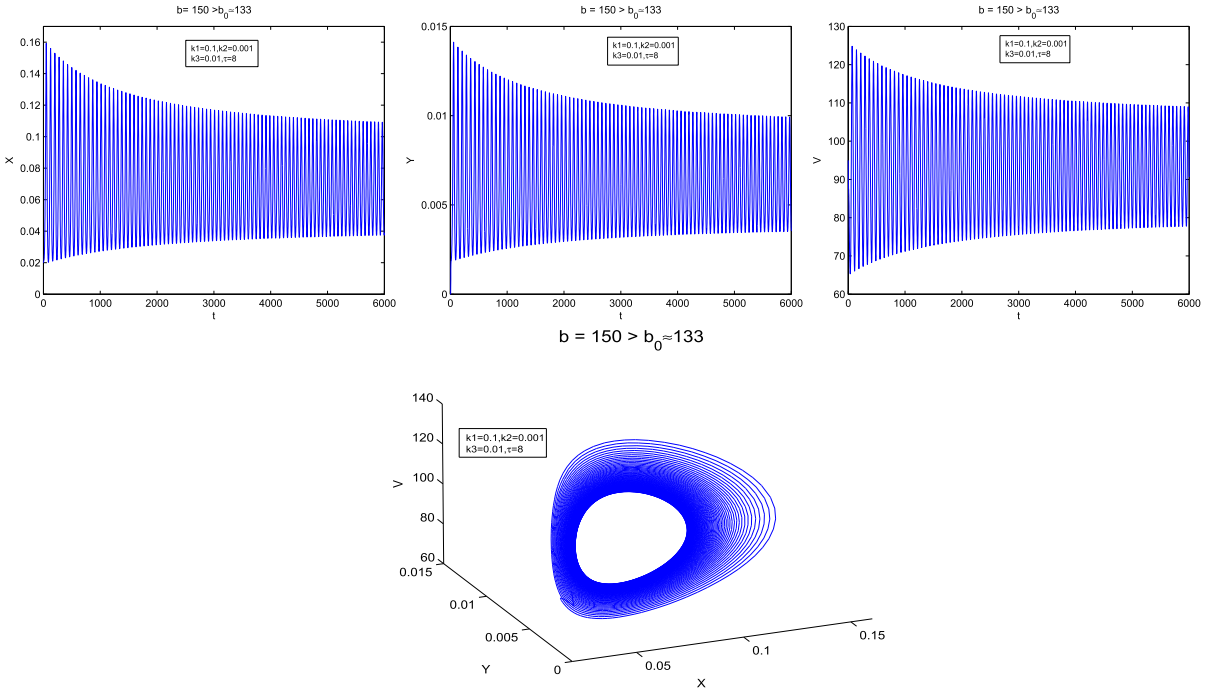

Fig. 7. Periodic solutions when $b > b^*$.

positive equilibrium solution E^*. For the value of b that is in the range between b_{c_1} and b_{c_2} for $\tau \geqslant 0$, the solution behavior is complicated by other model parameters. Recalling the ODE model [25] which does not have the period of the viral lytic cycle as a delay parameter, the dynamics is easier to characterize but may be insufficient to the real therapy. Concretely, in [25], it is shown that there also exist two threshold values for the burst size. Below the first threshold, the system has a globally asymptotically stable virus free equilibrium, this result also occurs in our present model (2.2), which means under this condition the virus-free equilibrium E_1 is robust [23]; while passing this threshold, there is a locally stable positive equilibrium. Above the second threshold, there exits one or three families of periodic solutions arising from Hopf bifurcations. Comparing with the model with more details of the viral lytic cycle, namely the period of the viral lytic cycle included in the present paper, the delay parameter of the period of the viral lytic cycle makes the model more realistic although the burst size seems to be a major parameter to determine the outcome of the virotherapy. This may provide more realistic suggestions for experimental and/or clinical virotherapy than the ODE model and the other simple ones.

As mentioned in Introduction, two types of viruses have been applied in experiments and/or clinical virotherapy, oncolytic wild viruses and gene-modified viruses. There are various genetic methods that can be used to modify the genomes of viruses so that the viruses have desired burst sizes [6]. For different viruses, their burst sizes may be modified according to their nature to obtain new viruses with various burst sizes. As we demonstrated, the burst size has effects on the period of viral lytic cycle, and thus affects the outcome of the virotherapy. It is clear that any oncolytic virus with small burst size, say smaller than the first threshold, can not eradicate the tumor, in stead, the tumor will grow to its maximum volume. When oncolytic viruses have a medium burst size, the outcome of the virotherapy could be the coexistence of three populations – tumor cell population, infected tumor cell population, and virus population, and this is determined by the period of the lytic cycle. When oncolytic viruses have large burst size, the outcome of the virotherapy could be the coexistence of three populations or the oscillation of three population. If viruses have huge burst size, the period of the viral lytic cycle will have less effect, and the averages of each population will have a small portion although most outcome will be oscillations of three populations. Since the success of the therapy is determined by detectability of tumor cells, it will be reasonable to apply oncolytic viruses with big burst size in the treatments. However, the stability in each case, coexistence and oscillations, should be broken away when the solution tends to reduce the amount of tumor cells. Overall, a clinic implication is that the period of the viral lytic cycle and the viral burst size should be modified simultaneously when a type of a virus is modified for oncolytic virotherapy, so that the period of viral lytic cycle and burst size are in a suitable range which can produce a desired outcome.

As a theoretical implication, the appearance of periodic solutions in the model with viral lytic cycle included may explain the periodic phenomena observed in [12,20,22] and other works. In [22], the model is for a specific virus measles and it has extra term for cell-to-cell fusion. Although the oscillation was observed, the authors attribute it to some combined parameter which do not have a clear biological significance. In [20], the models have immune cell population. The author had pointed out that the oscillation may caused by the interaction between immune cells and tumor cells. In other works, for

example, in papers [21,23,24], the models only have two populations, tumor cells and infected tumor cells. Although some unstable oscillations were observed in some of those models, we could not figure out a clear biological meaning. In our recently accepted work [26], we considered a quasi-equilibrium state study where we did not have free virus. We observed oscillation phenomenon. However, we could not explain the relation between the threshold values of τ and the burst size b. In our current work, our conclusion seems reasonable in terms of explaining biological observations in [12]. Comparing with all existing models for viral therapy, our current model reveals a striking feature that the critical value of the period of the viral lytic cycle is determined by the viral burst size. An important clinic implication is that the burst size should be carefully modified according to its effect on the lytic cycle when a type of a virus is modified for virotherapy, so that the period of the viral lytic cycle is in a suitable range which can break away the stability of the positive equilibria or periodic solutions.

Acknowledgment

This research is partially supported by the National Natural Science Foundation of China (No. 11031002) and by National Science Foundation of US (DMS-1216907). The authors thank colleague Kurt Williamson for providing reference about the time period of the lytic cycle. We also would like to thank the reviewers' constructive suggestions which have improved the presentation of the paper.

Appendix A. Direction and stability of the Hopf bifurcation

In Section 4, we obtain some conditions under which the system (2.3) undergoes Hopf bifurcations along the bifurcation curve. In this appendix we shall derive some formulae to compute the direction of the Hopf bifurcation and the stability of the bifurcating periodic solutions by using the normal form and center manifold theory [29].

Let $\tau = \tau_0 + \epsilon,\ \epsilon \in R$. Then $\epsilon = 0$ is the Hopf bifurcation value for system (2.3). Choosing the phase space as $C = C([-\tau, 0], R^3)$ then system (2.3) is transformed into an FDE in C.

$$\dot{u} = L_\epsilon(u_t) + F(\epsilon, u_t), \tag{5.1}$$

where $u_t = u(t+\theta) \in C$, and $L_\epsilon : C \to R^3,\ F : R \times C \to R^3$.

For $\phi = (\phi_1, \phi_2, \phi_3)^T \in C([-\tau, 0], R^3)$, let

$$L_\epsilon \phi = A_1 \phi(0) + B_1 \phi(-\tau), \tag{5.2}$$

where

$$A_1 = \begin{pmatrix} -k_1 x^* & -k_1 x^* & -k_2 x^* \\ 0 & -1 & 0 \\ -k_2 v^* & b & -(k_2 x^* + k_3) \end{pmatrix}, \quad B_1 = \begin{pmatrix} 0 & 0 & 0 \\ k_2 v^* & 0 & k_2 x^* \\ 0 & 0 & 0 \end{pmatrix}$$

and

$$F(\epsilon, \phi) = \begin{pmatrix} -k_1 \phi_1^2(0) - k_1 \phi_1(0)\phi_2(0) - k_2 \phi_1(0)\phi_3(0) \\ k_2 \phi_1(-\tau)\phi_3(-\tau) \\ -k_2 \phi_1(0)\phi_3(0) \end{pmatrix}.$$

By the Riesz representation theorem, there exists a matrix whose components are bounded variation functions $\eta(\theta, \epsilon)$ in $\theta \in [-\tau, 0]$, such that

$$L_\epsilon \phi = \int_{-\tau}^{0} d\eta(\theta, \epsilon)\phi(\theta) \quad \text{for } \phi \in C. \tag{5.3}$$

In fact, we can choose

$$\eta(\theta, \epsilon) = A_1 \zeta(\theta) - B_1 \zeta(\theta + \tau), \tag{5.4}$$

where

$$\zeta(\theta) = \begin{cases} 1, & \theta = 0, \\ 0, & \theta \neq 0. \end{cases} \tag{5.5}$$

Then (5.3) is satisfied. For $\phi \in C^1([-\tau, 0], R^3)$, define

$$A(\epsilon)\phi = \begin{cases} \frac{d\phi(\theta)}{d\theta}, & \theta \in [-\tau, 0), \\ \int_{-\tau}^{0} d\eta(s, \epsilon)\phi(s), & \theta = 0 \end{cases} \tag{5.6}$$

and

$$R(\epsilon,\phi)=\begin{cases}0, & \theta\in[-\tau,0),\\ F(\epsilon,\phi), & \theta=0.\end{cases} \tag{5.7}$$

Hence, we can rewrite (5.1) in the following form:

$$\dot{u}_t=A(\epsilon)u_t+R(\epsilon,u_t), \tag{5.8}$$

where

$$u=(u_1,u_2,u_3)^T, u_t=u(t+\theta)\quad \textit{for } \theta\in[-\tau,0).$$

For $\psi\in C^1([0,\tau],(R^3)^*)$, define

$$A^*\psi(s)=\begin{cases}-\frac{d\psi(s)}{d\,s}, & s\in(0,\tau],\\ \int_{-\tau}^{0}d\eta(t,0)\psi(-t), & s=0.\end{cases} \tag{5.9}$$

For ϕ and ψ, we define the bilinear form

$$\langle\psi,\phi\rangle=\bar{\psi}(0)\phi(0)-\int_{-\tau}^{0}\int_{\xi=0}^{\theta}\bar{\psi}(\xi-\theta)d\eta(\theta)\phi(\xi)d\xi, \tag{5.10}$$

where $\eta(\theta)=\eta(\theta,0)$. Then A^* and $A(0)$ are adjoint operators. By the results in Section 4, we assume that $\pm i\omega_0$ are eigenvalues of $A(0)$. Thus, they are also eigenvalues of A^*.

We define

$$q(\theta)=(1,q_1,q_2)^Te^{i\omega_0\theta},\quad q^*(s)=D(q_1^*,q_2^*,1)e^{i\omega_0 s}. \tag{5.11}$$

By direct computation, we have that

$$q_1=\frac{k_2v^*-k_1x^*-i\omega_0}{k_1x^*+(i\omega_0+1)e^{i\omega_0\tau_0}},$$

$$q_2=\frac{k_1k_2x^*v^*+(i\omega_0+1)(i\omega_0+k_1x^*)e^{i\omega_0\tau_0}}{k_1k_2x^{*2}+k_2x^*(i\omega_0+1)e^{i\omega_0\tau_0}},$$

$$q_1^*=\frac{k_2v^*(be^{i\omega_0\tau_0}-1+i\omega_0)}{(1-i\omega_0)(k_1x^*-i\omega_0)+k_1k_2x^*v^*e^{i\omega_0\tau_0}},$$

$$q_2^*=\frac{b(k_1x^*-i\omega_0)+k_1k_2x^*v^*}{(1-i\omega_0)(k_1x^*-i\omega_0)+k_1k_2x^*v^*e^{i\omega_0\tau_0}},$$

where $q(\theta)$ is the eigenvector of $A(0)$ corresponding to $i\omega_0$, and $q^*(s)$ is the eigenvector of A^* corresponding to $-i\omega_0$. Moreover,

$$\langle q^*,q\rangle=1,\quad \langle q^*,\bar{q}\rangle=0.$$

Then from (5.10), it follows that

$$\begin{aligned}\langle q^*(s),q(\theta)\rangle&=\bar{q}^*(0)q(0)-\int_{-\tau}^{0}\int_{\xi=0}^{\theta}\bar{q}^*(\xi-\theta)d\eta(\theta)q(\xi)d\xi\\ &=\bar{D}\{(\bar{q}_1^*,\bar{q}_2^*,1)(1,q_1,q_2)^T-\int_{-\tau}^{0}\int_{0}^{\theta}(\bar{q}_1^*,\bar{q}_2^*,1)e^{-i\omega_0(\xi-\theta)}d\eta(\theta)(1,q_1,q_2)^Te^{i\omega_0\xi}d\xi\}\\ &=\bar{D}\{\bar{q}_1^*+q_1\bar{q}_2^*+q_2-\int_{-\tau}^{0}(\bar{q}_1^*,\bar{q}_2^*,1)\theta e^{i\omega_0\theta}d\eta(\theta)(1,q_1,q_2)^T\}=\bar{D}\{\bar{q}_1^*+q_1\bar{q}_2^*+q_2+\tau k_2\bar{q}_2^*e^{-i\omega_0\tau}(v^*+q_2x^*)\}\\ &=1.\end{aligned}$$

Thus, we can choose $\bar{D}$ as

$$\bar{D}=\{\bar{q}_1^*+q_1\bar{q}_2^*+q_2+\tau k_2\bar{q}_2^*e^{-i\omega_0\tau}(v^*+q_2x^*)\}^{-1}.$$

Using the same notions as Hassard et al. [29], we first compute the coordinates to describe the center manifold C_0 at $\epsilon=0$.

Define

$$z(t)=\langle q^*(s),u_t(\theta)\rangle,\quad W(t,\theta)=u_t(\theta)-2Re\{z(t)q(\theta)\}.$$

On the center manifold C_0 we have

$$W(t,\theta)=W(z(t),\bar{z}(t),\theta),$$

where

$$W(t,\theta) = W_{20}(\theta)\frac{z^2}{2} + W_{11}(\theta)z\bar{z} + W_{02}(\theta)\frac{\bar{z}^2}{2} + \cdots,$$

z and $\bar{z}$ are local coordinates for center manifold C_0 in the direction of q^* and $\bar{q}^*$. Note that W is real if u_t is real. We only consider real solutions.

For solution $u_t \in C_0$ of system (2.3) with $\epsilon = 0$, then we have

$$\dot{z} = i\omega_0 z + \langle q^*(s), F(W + 2Re\{z(t)q(\theta)\})\rangle = i\omega_0 z + \bar{q}^*(0)F(W(z,\bar{z},0) + 2Re\{z(t)q(0)\}) = i\omega_0 z + \bar{q}^*(0)F_0(z,\bar{z}).$$

We rewrite this as

$$\dot{z} = i\omega_0 z(t) + g(z,\bar{z}), \tag{5.12}$$

where

$$g(z,\bar{z}) = \bar{q}^*(0)F_0(z,\bar{z}) = g_{20}(\theta)\frac{z^2}{2} + g_{11}(\theta)z\bar{z} + g_{02}(\theta)\frac{\bar{z}^2}{2} + g_{21}\frac{z^2\bar{z}}{2} + \cdots \tag{5.13}$$

By (5.8) and (5.12) we have

$$\begin{aligned}\dot{W} = \dot{u}_t - \dot{z}q - \dot{\bar{z}}\bar{q} &= \begin{cases} AW - 2Re\{\bar{q}^*(0)F_0 q(\theta)\}, & \theta \in [-\tau, 0), \\ AW - 2Re\{\bar{q}^*(0)F_0 q(\theta)\} + F_0, & \theta = 0, \end{cases} \\ &= AW + H(z,\bar{z},\theta),\end{aligned}$$

where

$$H(z,\bar{z},\theta) = H_{20}(\theta)\frac{z^2}{2} + H_{11}(\theta)z\bar{z} + H_{02}(\theta)\frac{\bar{z}^2}{2} + \cdots \tag{5.14}$$

Expanding and comparing the coefficients, we obtain

$$(A - 2i\omega_0)W_{20}(\theta) = -H_{20}(\theta), AW_{11}(\theta) = -H_{11}(\theta), (A + 2i\omega_0)W_{02}(\theta) = -H_{02}(\theta), \cdots \tag{5.15}$$

Notice that

$$u_{1t}(0) = z + \bar{z} + W_{20}^{(1)}(0)\frac{z^2}{2} + W_{11}^{(1)}(0)z\bar{z} + W_{02}^{(1)}(0)\frac{\bar{z}^2}{2} + \cdots,$$

$$u_{2t}(0) = q_1 z + \bar{q}_1\bar{z} + W_{20}^{(2)}(0)\frac{z^2}{2} + W_{11}^{(2)}(0)z\bar{z} + W_{02}^{(2)}(0)\frac{\bar{z}^2}{2} + \cdots,$$

$$u_{3t}(0) = q_2 z + \bar{q}_2\bar{z} + W_{20}^{(3)}(0)\frac{z^2}{2} + W_{11}^{(3)}(0)z\bar{z} + W_{02}^{(3)}(0)\frac{\bar{z}^2}{2} + \cdots,$$

$$u_{1t}(-\tau) = e^{-i\omega_0\tau}z + e^{i\omega_0\tau}\bar{z} + W_{20}^{(1)}(-\tau)\frac{z^2}{2} + W_{11}^{(1)}(-\tau)z\bar{z} + W_{02}^{(1)}(-\tau)\frac{\bar{z}^2}{2} + \cdots,$$

$$u_{3t}(-\tau) = q_2 e^{-i\omega_0\tau}z + \bar{q}_2 e^{i\omega_0\tau}\bar{z} + W_{20}^{(3)}(-\tau)\frac{z^2}{2} + W_{11}^{(3)}(-\tau)z\bar{z} + W_{02}^{(3)}(-\tau)\frac{\bar{z}^2}{2} + \cdots$$

and

$$F_0 = \begin{pmatrix} -k_1 u_{1t}^2(0) - k_1 u_{1t}(0)u_{2t}(0) - k_2 u_{1t}(0)u_{3t}(0) \\ k_2 u_{1t}(-\tau)u_{3t}(-\tau) \\ -k_2 u_{1t}(0)u_{3t}(0) \end{pmatrix},$$

we have

$$\begin{aligned} g(z,\bar{z}) &= \bar{q}^*(0)F_0 \\ &= \bar{D}(\bar{q}_1^*, \bar{q}_2^*, 1)\begin{pmatrix} -k_1 u_{1t}^2(0) - k_1 u_{1t}(0)u_{2t}(0) - k_2 u_{1t}(0)u_{3t}(0) \\ k_2 u_{1t}(-\tau)u_{3t}(-\tau) \\ -k_2 u_{1t}(0)u_{3t}(0) \end{pmatrix} \\ &= \bar{D}\{\bar{q}_1^*[-k_1 u_{1t}^2(0) - k_1 u_{1t}(0)u_{2t}(0) - k_2 u_{1t}(0)u_{3t}(0)] + \bar{q}_2^* k_2 u_{1t}(-\tau)u_{3t}(-\tau) - k_2 u_{1t}(0)u_{3t}(0)\}. \end{aligned}$$

Comparing the coefficients with (5.13), we have

$$g_{20} = 2\bar{D}(-k_1\bar{q}_1^* - k_1 q_1\bar{q}_1^* - k_2\bar{q}_1^* q_2 + q_2\bar{q}_2^* e^{-2i\omega_0\tau} - k_2 q_2),$$

$$g_{11} = \bar{D}(-2k_1\bar{q}_1^* - k_1\bar{q}_1\bar{q}_1^* - k_1q_1\bar{q}_1^* - k_2\bar{q}_1^*\bar{q}_2 - k_2\bar{q}_1^*q_2 + k_2\bar{q}_2\bar{q}_2^* + k_2q_2\bar{q}_2^* - k_2q_2 - k_2\bar{q}_2),$$

$$g_{02} = 2\bar{D}(-k_1\bar{q}_1^* - k_1q_1\bar{q}_1^* - k_2\bar{q}_1^*\bar{q}_2 + k_2\bar{q}_2\bar{q}_2^*e^{2i\omega_0\tau} - k_2\bar{q}_2),$$

$$\begin{aligned} g_{21} = \bar{D}[&(-2k_1\bar{q}_1^* - k_1\bar{q}_1\bar{q}_1^* - k_2\bar{q}_1^*\bar{q}_2 - k_2\bar{q}_2)W_{20}^{(1)}(0) + (-4k_1\bar{q}_1^* - 2k_1q_1\bar{q}_1^* - 2k_2\bar{q}_1^*q_2 - 2k_2q_2)W_{11}^{(1)}(0) - k_1\bar{q}_1^*W_{20}^{(2)}(0) \\ &- 2k_1\bar{q}_1^*W_{11}^{(2)}(0) - k_2(\bar{q}_1^* + 1)W_{20}^{(3)}(0) - 2k_2(\bar{q}_1^* + 1)W_{11}^{(3)}(0) + k_2\bar{q}_2\bar{q}_2^*e^{i\omega_0\tau}W_{20}^{(1)}(-\tau) + 2k_2q_2\bar{q}_2^*e^{-i\omega_0\tau}W_{11}^{(1)}(-\tau) \\ &+ k_2\bar{q}_2^*e^{i\omega_0\tau}W_{20}^{(3)}(-\tau) + 2k_2\bar{q}_2^*e^{-i\omega_0\tau}W_{11}^{(3)}(-\tau)]. \end{aligned}$$

We still need to compute $W_{20}(\theta)$ and $W_{11}(\theta)$ for $\theta \in [-\tau, 0)$. We have

$$H(z, \bar{z}, \theta) = -2Re\{\bar{q}^*(0)F_0q(\theta)\} = -gq(\theta) - \bar{g}\bar{q}(\theta).$$

Comparing the coefficients with (5.14), we get

$$H_{20}(\theta) = -g_{20}q(\theta) - \bar{g}_{02}\bar{q}(\theta),$$

$$H_{11}(\theta) = -g_{11}q(\theta) - \bar{g}_{11}\bar{q}(\theta).$$

It follows from (5.15) that

$$\dot{W}_{20}(\theta) = 2i\omega_0W_{20}(\theta) + g_{20}q(\theta) + \bar{g}_{02}\bar{q}(\theta).$$

Solving for $W_{20}(\theta)$, we obtain

$$W_{20}(\theta) = \frac{ig_{20}}{\omega_0}q(\theta) + \frac{i\bar{g}_{02}}{3\omega_0}\bar{q}(\theta) + E_1e^{2i\omega_0\theta} \tag{5.16}$$

and similarly

$$W_{11}(\theta) = -\frac{ig_{11}}{\omega_0}q(\theta) + \frac{i\bar{g}_{11}}{\omega_0}\bar{q}(\theta) + E_2, \tag{5.17}$$

where E_1 and E_2 are both 3-dimensional vectors which can be determined by setting $\theta = 0$ in H. In fact, since

$$H(z, \bar{z}, \theta) = -2Re\{\bar{q}^*(0)F_0q(\theta)\} + F_0,$$

we have

$$H_{20}(0) = -g_{20}q(0) - \bar{g}_{02}\bar{q}(0) + F_{z^2}, \tag{5.18}$$

$$H_{11}(0) = -g_{11}q(0) - \bar{g}_{11}\bar{q}(0) + F_{z\bar{z}}, \tag{5.19}$$

where

$$F_0 = F_{z^2}\frac{z^2}{2} + F_{z\bar{z}}z\bar{z} + F_{\bar{z}^2}\frac{\bar{z}^2}{2} + \cdots,$$

$$F_{z^2} = \begin{pmatrix} -2k_1 - 2k_1q_1 - 2k_2q_2 \\ 2k_2q_2e^{-2i\omega_0\tau} \\ -2k_2q_2 \end{pmatrix},$$

$$F_{z\bar{z}} = \begin{pmatrix} -2k_1 - k_1(q_1 + \bar{q}_1) - k_2(q_2 + \bar{q}_2) \\ k_2(q_2 + \bar{q}_2) \\ -k_2(q_2 + \bar{q}_2) \end{pmatrix},$$

$$F_{\bar{z}^2} = \begin{pmatrix} -2k_1 - 2k_1\bar{q}_1 - 2k_2\bar{q}_2 \\ 2k_2\bar{q}_2e^{2i\omega_0\tau} \\ -2k_2\bar{q}_2 \end{pmatrix}.$$

Hence, from combining the definition of A, we can get

$$\int_{-\tau}^{0} d\eta(\theta)W_{20}(\theta) = AW_{20}(0) = 2i\omega_0W_{20}(0) + g_{20}q(0) + \bar{g}_{02}\bar{q}(0) - F_{z^2} \tag{5.20}$$

and

$$\int_{-\tau}^{0} d\eta(\theta)W_{11}(\theta) = AW_{11}(0) = g_{11}q(0) + \bar{g}_{11}\bar{q}(0) - F_{z\bar{z}}. \tag{5.21}$$

Notice that

$$\left[i\omega_0 I - \int_{-\tau}^{0} e^{i\omega_0\theta} d\eta(\theta)\right] q(0) = 0, \tag{5.22}$$

$$\left[-i\omega_0 I - \int_{-\tau}^{0} e^{-i\omega_0\theta} d\eta(\theta)\right] \bar{q}(0) = 0. \tag{5.23}$$

Substituting (5.16) and (5.18) into (5.20), we obtain

$$\left[2i\omega_0 I - \int_{-\tau}^{0} e^{2i\omega_0\theta} d\eta(\theta)\right] E_1 = F_{z^2}. \tag{5.24}$$

Similarly, we have

$$\left[\int_{-\tau}^{0} d\eta(\theta)\right] E_2 = -F_{z\bar{z}}. \tag{5.25}$$

Hence we obtain

$$\begin{pmatrix} 2i\omega_0 + k_1 x^* & k_1 x^* & k_2 x^* \\ -k_2 v^* e^{-2i\omega_0\tau} & 2i\omega_0 + 1 & -k_2 x^* e^{-2i\omega_0\tau} \\ k_2 v^* & -b & 2i\omega_0 + k_2 x^* + k_3 \end{pmatrix} E_1 = 2 \begin{pmatrix} -k_1 - k_1 q_1 - k_2 q_2 \\ k_2 q_2 e^{-2i\omega_0\tau} \\ -k_2 q_2 \end{pmatrix}$$

and

$$\begin{pmatrix} k_1 x^* & k_1 x^* & k_2 x^* \\ -k_2 v^* & 1 & -k_2 x^* \\ k_2 v^* & -b & k_2 x^* + k_3 \end{pmatrix} E_2 = \begin{pmatrix} 2k_1 + k_1(q_1 + \bar{q}_1) + k_2(q_2 + \bar{q}_2) \\ -k_2(q_2 + \bar{q}_2) \\ k_2(q_2 + \bar{q}_2) \end{pmatrix}.$$

We can determine $W_{20}(\theta)$, $W_{11}(\theta)$ from (5.16) and (5.17), then g_{21} can be expressed. Since each g_{ij} is determined by the parameter and delays in system (2.3), we can compute the following quantities:

$$\begin{aligned} c_1(0) &= \frac{i}{2\omega_0}\left(g_{20}g_{11} - 2|g_{11}|^2 - \frac{1}{3}|g_{02}|^2\right) + \frac{1}{2}g_{21}, \\ \mu_2 &= -\frac{\mathrm{Re}\{c_1(0)\}}{\mathrm{Re}\{\mu'(\tau_0)\}}, \\ T_2 &= -\frac{1}{\omega_0}(\mathrm{Im}\{c_1(0)\} + \mu_2 \mathrm{Im}\{\mu'(\tau_0)\}), \\ \beta_2 &= 2\mathrm{Re}\{c_1(0)\}. \end{aligned} \tag{5.26}$$

We know that (see [29]) μ_2 determines the directions of the Hopf bifurcation: if $\mu_2 > 0$ (< 0), the bifurcating periodic solutions exists in a right (left) neighborhood of τ_0; β_2 determines the stability of the bifurcating periodic solutions: the bifurcating periodic solutions are orbitally stable (unstable) if $\beta_2 < 0$ (> 0); and T_2 determines the period of the bifurcation periodic solutions: the period increase (decrease) if $T_2 > 0$ (< 0).

References

[1] E. Kelly, S. Russell, History of oncolytic viruses: genesis and genetic engineering, Mol. Ther. 15 (4) (2007) 651–659.
[2] D.H. Kirn, F. McCormick, Replicating viruses as selective cancer therapeutics, Mol. Med. Today 2 (1996) 519–527.
[3] M.S. Roberts, R.M. Lorence, W.S. Groene, M.K. Bamat, Naturally oncolytic viruses, Curr. Opin. Mol. Ther. 8 (2006) 314–321.
[4] J.M. Kaplan, Adenovirus-based cancer gene therapy, Curr. Gene. Ther. 5 (2005) 595–605.
[5] D. Cervantes-Garcia, R. Ortiz-Lopez, N. Mayek-Perez, A. Rojas-Martinez, Oncolytic virotherapy, Ann. Hepatol. 7 (2008) 34–45.
[6] E.A. Chicca, Oncolytic viruses, Nat. Rev. Cancer 2 (2002) 938–950.
[7] M. Madigan, J. Martinko (Eds.), Brock Biology of Microorganisms, eleventh ed., Prentice Hall, 2006.
[8] A.R. Hall, B.R. Dix, S.J. O'Carroll, A.W. Braithwaite, p53-Dependent cell death/apoptosis is required for a productive adenovirus infection, Nat. Med. 4 (1998) 1068–1072.
[9] J.N. Harada, A.J. Berk, p53-Independent and -dependent requirements for E1B-55k in adenovirus type 5 replication, J. Virol. 73 (1999) 5333–5344.
[10] B.R. Dix, S.J. O'Carroll, C.J. Myers, S.J. Edwards, A.W. Baithwaite, Efficient induction of cell death by adenoviruses requires binding of E1B and p53, Cancer Res. 60 (2000) 2666–2672.
[11] M. Ramachandra et al, Re-engineering adenovirus regulatory pathways to enhance oncolytic specificity and efficacy, Nat. Biotechnol. 19 (2001) 1035–1041.
[12] E.A. Chiocca, K.M. Abbed, S. Tatter, et al, A phase I openlabel,dose-escalation, multi-institutional trial of injection with an E1B-attenuated adenovirus, ONYX-015 into the peritumoral region of recurrent malignant gliomas in the adjuvant setting, Mol Ther. 10 (2004) 958–966.
[13] R.M. Lorence, A.L. Pecora, P.P. Major, et al, Overview of phase I studies of intravenous administration of PV701, an oncolytic virus, Curr. Opin. Mol. Ther. 5 (2003) 618–624.
[14] V. Papanastassiou, R. Rampling, M. Fraser, et al, The potential for efficacy of the modified (ICP 34.5(-)) herpes simplex virus HSV1716 following intratumoural injection into human malignant glioma: a proof of principle study, Gene Ther. 9 (2002) 398–406.

[15] A.L. Pecora, N. Rizvi, G.I. Cohen, et al, Phase I trial of intravenous administration of PV701, an oncolytic virus in patients with advanced solid cancers, J. Clin. Oncol. 20 (2002) 2251–2266.
[16] J. Wu, H. Byrne, D. Kirn, L.M. Wein, Modeling and analysis of a virus that replicates selectively in tumor cells, Bull. Math. Biol. 63 (4) (2001) 731–768.
[17] L.M. Wein, J.T. Wu, D.H. Kirn, Validation and analysis of a mathematical model of a replication-competent oncolytic virus for cancer treatment: implications for virus design and delivery, Cancer Res. 63 (6) (2003) 1317–1324.
[18] Y. Tao, Q. Guo, The competitive dynamics between tumor cells, a replication-competent virus and an immune response, J. Math. Biol. 51 (1) (2005) 37–74.
[19] A. Friedman, J.P. Tian, G. Fulci, E. A Chiocca, J. Wang, Glioma virotherapy: effects of innate immune suppression and increased viral replication capacity, Cancer Res. 66 (4) (2006) 2314–2319.
[20] D. Wodarz, Viruses as antitumor weapons: defining conditions for tumor remission, Cancer Res. 61 (2001) 3501–3507.
[21] A.S. Novozhilov, F.S. Berezovskaya, E.V. Koonin, G.P. Karev, Mathematical modeling of tumor therapy with oncolytic viruses: regimes with complete tumor elimination within the framework of deterministic models, Biol. Direct. 1 (2006) 1–6.
[22] Z. Bajzer, T. Carr, K. Josic, S.J. Russell, D. Dingli, Modeling of cancer virotherapy with recombinant measles viruses, J. Theor. Biol. 252 (1) (2008) 109–122.
[23] N. Komarova, D. Wodarz, ODE models for oncolytic virus dynamics, J. Theor. Biol. 263 (2010) 530–543.
[24] D. Wodarz, N. Komarova, Towards predictive computational models of oncolytic virus therapy: basis for experimental validation and model selection, PloS ONE 4 (1) (2009) e4271.
[25] J.P. Tian, The replicability of oncolytic virus: defining conditions in tumor virotherapy, Math. Biosci. Eng. 8 (3) (2011) 841–860.
[26] J.P. Tian, Y. Kuang, H. Yang, Intracellular viral life-cycle induced rich dynamics in tumor virotherapy, Can. Appl. Math. Q., in press.
[27] J. LaSalle, S. Lefschetz, Stability by Lyapunov's Direct Method, Academic Press, New York, 1961.
[28] S. Ruan, J. Wei, On the zeros of third degree exponential polynomial with applications to a delayed model for the control of testosterone secretion, IMA J. Math. Appl. Med. Biol. 18 (2001) 41–52.
[29] B.D. Hassard, N.D. Kazarinoff, Y.H. Wan, Theory and Applications of Hopf Bifurcation, Cambridge University Press, Cambridge, 1981.